

Frustrated Cooper pairing and the *f*-wave supersolidity

Hsiang-Hsuan Hung,¹ Wei-Cheng Lee,¹ and Congjun Wu¹

¹*Department of Physics, University of California, San Diego, CA 92093*

(Dated: February 3, 2019)

Geometric frustration in quantum magnetism refers to that magnetic interactions on different bonds cannot be simultaneously minimized. The usual Cooper pairing systems favor the uniform distribution of the pairing phase among lattice sites without frustration. In contrast, we propose “frustrated Cooper pairing” in non-bipartite lattices which leads to frustrated supersolid states with non-uniform distributions of the Cooper pair phase and density. This exotic pairing state naturally occurs in the *p*-orbital band in optical lattices with ultra-cold spinless fermions. In the triangular lattice, it exhibits an unconventional supersolid state with the *f*-wave symmetry.

PACS numbers: 03.75.Ss, 75.50Cc, 03.75mn, 71.10.Fd, 05.50.+q

Frustration is one of the fundamental challenges in classic and quantum magnetism [1]. For the antiferromagnetic states in non-bipartite lattices, such as triangular, Kagome and pyrochlore, it is impossible to simultaneously minimize the magnetic energy of each bond. This results in the high degeneracy of the ground state configurations which gives rise to the enhanced thermal and quantum fluctuations strongly suppressing spin ordering. Frustration provides a promising way to reach the spin liquid states, which exhibit exotic properties including topological ordering and fractionalization [2, 3].

In the usual superfluid states of paired fermions and bosons, frustration does not play a role. In order to maximally facilitate phase coherence, a uniform distribution of the superfluid phase over the lattice sites is favored. Remarkably, the striped superconductivity [4, 5], which is beyond this paradigm, has been proposed for the high T_c compound $\text{La}_{2-x}\text{Ba}_x\text{CuO}_4$. The Josephson coupling between two adjacent superconducting stripes is like in the π -junction leading to the opposite signs of the pairing phases across the junction. The mechanism for the frustrated coupling may arise from the interplay between superconductivity and antiferromagnetism in doped Mott insulators. However, a clear understanding of the microscopic origin of this phase is still needed.

On the other hand, cold atom optical lattices have opened up a new opportunity to investigate novel features of orbital physics which do not exhibit in usual orbital systems of transition metal oxides. Bosons have been pumped into the excited *p*-orbital bands experimentally with a long life time[6]. This metastable excited state of bosons does not obey the “no-node” theory and exhibits the unconventional superfluidity with complex-valued many-body wavefunctions breaking time-reversal symmetry spontaneously [7, 8, 9, 10]. For orbital fermions, large progress has been made in the *p_{x,y}*-orbital bands in the hexagonal lattices, whose physics is fundamentally different from that in the *p_z*-orbital system of graphene. The interesting physics includes the flat band structure [11], the consequential non-perturbative strong correlation effects (e.g. Wigner crystal [12] and ferro-

magnetism [13]), frustrated orbital exchange interaction [14], quantum anomalous Hall effect [15], and the unconventional *f*-wave Cooper pairing [16].

In this article, we bridge the above important research directions together by introducing frustration to Cooper pairing as a new feature of orbital physics. We propose the “frustrated Cooper pairing” in the *p_{x,y}*-band of the non-bipartite optical lattices with spinless fermions. Due to the odd parity nature of the *p_{x,y}*-orbitals, the Josephson coupling of the on-site Cooper pairing is frustrated. In the strong coupling limit, the super-exchange interaction of the pseudo-spin algebra composed of the pairing and density operators is described by the “antiferromagnetic” Heisenberg model with the Ising anisotropy. It results in the coexistence of charge density wave and superfluidity of Cooper pairs with a non-uniform phase pattern. This supersolid state of Cooper pairs exhibits the *f*-wave pairing symmetry in the triangular lattice within a large range of particle density.

We take the 2D triangular lattice as an example, which has been constructed experimentally by three coplanar laser beams [17]. The optical potential on each site is approximated by a 3D anisotropic harmonic potential with frequencies $\omega_z \gg \omega_x = \omega_y$. After the lowest *s*-band is fulfilled, the active orbital bands become *p_{x,y}*. The *p_z*-band remains empty and is neglected. The free part of the *p_{x,y}*-orbital band Hamiltonian in the triangular lattice filled with spinless fermions reads

$$H_0 = t_{\parallel} \sum_{\vec{r}, i=1 \sim 3, \sigma} (p_{L, \vec{r}, i}^\dagger p_{L, \vec{r}+a\hat{e}_i, i} + h.c.) - t_{\perp} \sum_{\vec{r}, i=1 \sim 3, \sigma} (p_{T, \vec{r}, i}^\dagger p_{T, \vec{r}+a\hat{e}_i, i} + h.c.) - \mu \sum_{\vec{r}\sigma} n_{\vec{r}\sigma}, \quad (1)$$

where \vec{r} runs over all the sites; $\hat{e}_1 = \hat{e}_x$, $\hat{e}_{2,3} = -\frac{1}{2}\hat{e}_x \pm \frac{\sqrt{3}}{2}\hat{e}_y$ are the three unit vectors along bond directions; a is the lattice constant; $p_{L, i} \equiv (p_x \hat{e}_x + p_y \hat{e}_y) \cdot \hat{e}_i$ are the longitudinal projections of the *p*-orbitals along the \hat{e}_i direction; $p_{T, i} \equiv (p_x \hat{e}_x + p_y \hat{e}_y) \cdot (\hat{z} \times \hat{e}_i)$ are the transverse projections of the *p*-orbitals; $n_{\vec{r}} = p_x^\dagger p_x + p_y^\dagger p_y$ is

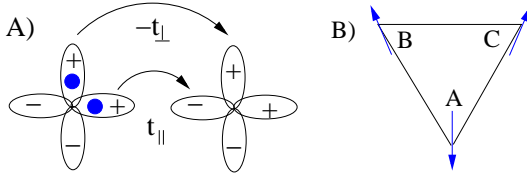


FIG. 1: A) The odd parity of the p -orbitals gives rise to the “antiferromagnetic”-like Heisenberg model of the pseudospin $\vec{\eta}$ vector, which is frustrated in the triangular lattice. B) The pattern of $\langle G|\vec{\eta}|G\rangle$ at $h=0$: the unit cell of three sites exhibiting the supersolid ordering.

the particle number operator; μ is the chemical potential. The σ -bonding t_{\parallel} and π -bonding t_{\perp} describe the hoppings between p -orbitals along and perpendicular to the bond direction, respectively. t_{\parallel} is positive due to the odd parity nature of the p -orbitals. t_{\perp} is usually much smaller than t_{\parallel} because of the anisotropy of the p -orbitals. We consider the Hubbard attractive interaction between spinless fermions in the $p_{x,y}$ -orbital bands

$$H_{int} = -U \sum_{\vec{r}} n_{\vec{r},p_x} n_{\vec{r},p_y}, \quad (2)$$

where U is positive.

The frustrated nature of Cooper pairing can be easily explained in the strong coupling limit of $U \gg t_{\parallel}$. The low energy Hilbert space in each site consists of the doubly occupied state and the empty state, which play the roles of “up” and “down” states respectively, for the well-known pseudospin algebra denoted as $\eta_x = \frac{1}{2}(p_x^\dagger p_y^\dagger + p_y p_x)$, $\eta_y = -\frac{i}{2}(p_x^\dagger p_y^\dagger - p_y p_x)$, $\eta_z = \frac{1}{2}(n_{\vec{r}} - 1)$. Up to a normalization factor, they are the real and imaginary parts of the pairing operator, and the particle density operator, respectively. This super-exchange interaction of the pseudo-spin has a remarkable feature that a π -phase difference is favored between pairing order parameters $\eta_{x,y}$ on neighboring sites. As a pair hops to the neighboring site, it gains a π -phase shift as depicted in Fig. 1 A, because the σ -bonding and π -bonding terms are with opposite signs. The perturbation theory gives rise to the anisotropic “antiferromagnetic” Heisenberg model (AAFHM) in the “external magnetic field”,

$$H_{eff} = \sum_{ij} J_{x,y} \{ \eta_x(i) \eta_x(j) + \eta_y(i) \eta_y(j) \} + J_z \eta_z(i) \eta_z(j) - h \sum_i \eta_z(i), \quad (3)$$

where $J_{x,y} = (4t_{\perp}t_{\parallel})/U$ and $J_z = [2(t_{\perp}^2 + t_{\parallel}^2)]/U$, $h = 2\mu$ is the external magnetic field. The Ising anisotropy in Eq. 3 is because $J_z \geq J_{x,y}$. Similar models apply to pairing problem of spinless fermions in the $p_{x,y}$ -orbital of the bipartite lattices of square [18] and hexagonal [16] which are not frustrated because a canonical transformation can change $J_{x,y}$ to $-J_{x,y}$.

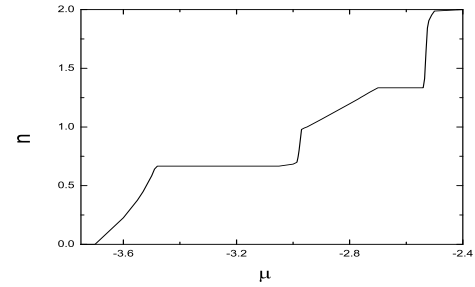


FIG. 2: The average fermion number per site n versus the chemical potential μ at $U/t_{\parallel} = 6$ and $t_{\perp}/t_{\parallel} = 0.2$.

Eq. 3 can be interpreted as a hard core boson model with the frustrated hopping $J_{x,y}$ and the nearest neighbor repulsion J_z . It has been studied at the zero external field in Ref. [19, 20] which shows a supersolid ordering with a three-site unit cell as depicted in Fig. 1 B. Site A has no superfluid component, *i.e.*, $\vec{\eta} \parallel \hat{z}$; sites B and C develop superfluid orders with a π -phase difference. However, the experimental realization of hard core bosons with frustrated hopping is difficult. In comparison, our idea of the frustrated Cooper pairing of fermions is very natural in the $p_{x,y}$ -orbital bands. Furthermore, previous studies [19, 20] focus on the pseudo-spin model Eq. 3 completely neglecting the fermion degree of freedom. In the following, instead of using Eq. 3, we directly study the Cooper pairing problem with the fermion Hamiltonian in the entire filling range from 0 to 2.

Next we perform the self-consistent mean-field theory to Eq. 1 and Eq. 2. To decouple H_{int} , we assume the pairing and charge density wave (CDW) ordering taking an enlarge unit cell of three sites, and define $\Delta_I = \langle G|p_{\vec{r} \in I,y} p_{\vec{r} \in I,x}|G\rangle$ and $N_I = \frac{1}{2}\langle G|\hat{n}_{\vec{r} \in I}|G\rangle$ where $I = A, B, C$ refer to the sublattice index; $\langle G|...|G\rangle$ means the average over the mean-field ground state. The mean-field interaction Hamiltonian becomes:

$$H_{int}^{mf} = -U \sum_{\vec{r}, I=A,B,C} \{ \Delta_I^* p_{\vec{r} \in I,y} p_{\vec{r} \in I,x} + h.c. \} + N_I \{ p_{\vec{r} \in I,x}^\dagger p_{\vec{r} \in I,x} + p_{\vec{r} \in I,y}^\dagger p_{\vec{r} \in I,y} \} \quad (4)$$

Combining Eqs. 1 and 4 and performing Fourier transformation to momentum space, we can obtain the resulting mean-field Hamiltonian as:

$$H = \sum'_{\vec{k}} \hat{\Psi}^\dagger(\vec{k}) \begin{pmatrix} \hat{H}_s(\vec{k}) & \hat{D}(\vec{k}) \\ \hat{D}^\dagger(\vec{k}) & -\hat{H}_s^*(-\vec{k}) \end{pmatrix} \hat{\Psi}(\vec{k}) \quad (5)$$

where $\sum'_{\vec{k}}$ means the summation only cover half of the reduced Brillouin zone; $\hat{\Psi}(\vec{k}) = (\phi(\vec{k})^T, \phi(-\vec{k})^\dagger)$, and $\phi(\vec{k}) = [p_{A,x}(\vec{k}), p_{A,y}(\vec{k}), p_{B,x}(\vec{k}), p_{B,y}(\vec{k}), p_{C,x}(\vec{k}), p_{C,y}(\vec{k})]$. H_s contains the free Hamiltonian Eq. 1 combined with

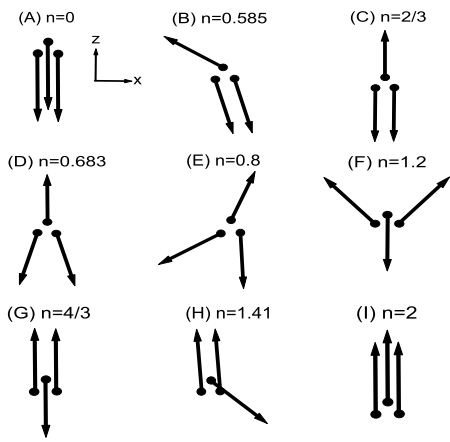


FIG. 3: The real space configurations of pseudospin $\vec{\eta}$ on the xz plane at various fillings n from (A) to (I). A) and (I) indicate fully polarized states. (B) and (H) show three tilted vectors, where two of them have a relative π -phase to the third one. (C) and (G) depict the CDW insulating state. (D) and (F) exhibit an umbrella-like shape with opposite orientation. Two of them have a π -phase difference and the third one does not own superfluid component. (E) denotes an intermediate configuration between (D) and (F).

the CDW decoupling; $D(\vec{k})$ is the pairing part. The order parameters are obtained self-consistently. The above definition of order parameters are related to the pseudospin operators through

$$\begin{aligned} \langle G|\eta_x(\vec{r} \in I)|G\rangle &= \text{Re}\Delta_I, \quad \langle G|\eta_y(\vec{r} \in I)|G\rangle = \text{Im}\Delta_I, \\ \langle G|\eta_z(\vec{r} \in I)|G\rangle &= N_I - 1/2. \end{aligned} \quad (6)$$

Different from the ordinary BCS problem, the pairing of Eq. 1 is not an infinitesimal instability but occurs at the finite attraction strength. It is because the eigenstates of the two time-reversal partners with momentum \vec{k} and $-\vec{k}$ of the free Hamiltonian Eq. 1 have the same real polar orbital configuration. This suppresses pairing at weak interactions because attraction only exists in orthogonal orbitals. With intermediate and strong interactions, the band structure is significantly modified and Cooper pairing develops. Below we present results for $t_{\perp}/t_{\parallel} = 0.2$ and an intermediate coupling and $U/t_{\parallel} = 6$. This corresponds to the effective AAFHM with the Ising anisotropy of $J_z/J_{x,y} = 2.6$.

We discuss our mean-field results in terms of the pseudospin orientations at the three sublattices A, B, C . Fig. 2 shows the total fermion number per site $n = (n_A + n_B + n_C)/3$ as a function of chemical potential μ , which is the counterpart of the magnetization in the AAFHM. The first prominent feature is the plateaus occurring at $n = \frac{2}{3}$ and $\frac{4}{3}$, which is corresponding to those at $\langle G|\eta_z|G\rangle = \pm\frac{1}{3}$ observed in the study of classical ground state of the

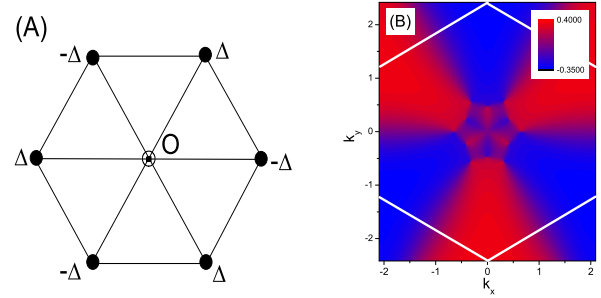


FIG. 4: The f -wave pairing pattern in (A) real space and (B) momentum space. The rotation of 60° around the center site O in A) (denoted by the hollow circle) in real space or around the center of the reduced BZ in momentum space is equivalent to reverse the sign of the pairing order parameters.

AAFHM. These two plateaus are corresponding to CDW insulating states without superfluidity. As shown in Fig. 3, the corresponding pseudospin orientation for CDW insulating states is that all the pseudospins are fully polarized along the \hat{z} axis with two of sublattice along the same direction and the remaining one along the opposite direction.

Although Fig. 2 resembles the behaviors of the magnetization obtained by the AAFHM [21], two major differences exist. First, the widths of the two CDW plateaus in Fig. 2 are different while those of the AAFHAM are the same. We attribute this discrepancy to the different symmetry properties between the AAFHM and the Hubbard model of Eq. 1 and Eq. 2. The AAFHM has the symmetry of the rotation of 180° around the x -axis, *i.e.*, $\eta_x \rightarrow \eta_x$, $\eta_y, \eta_z \rightarrow -\eta_y, -\eta_z$ and $h \rightarrow -h$. Such an operator corresponds to the particle-hole transformation at the fermion level as $p_x \rightarrow ip_y^\dagger$ and $p_y^\dagger \rightarrow ip_x$, which is not kept in the triangular lattice. As a result, for the AAFHM, the magnetization should be an odd function with respect to h so that the lengths of the plateaus are the same. This kind of behavior is not expected in Fig. 2. The other difference is that at $h = 0$, the ferrimagnetic state is found in the AAFHM, and our results show the 'paramagnetic' behavior, *i.e.*, there is no jump around $n = 1$. This is due to the quantum fluctuations arising from the singly occupied states as discussed below.

Fig. 3 plots the pseudospin orientations on three sublattices at some representative filling levels. Except the CDW insulating states at $n = \frac{2}{3}, \frac{4}{3}$, we find that the pseudospins have non-zero $\langle G|\eta_x|G\rangle$ and $\langle G|\eta_z|G\rangle$ in the most part of the phase diagram, indicating the frustrated supersolid states with non-uniform Cooper pairing density and phase. Moreover, the phase diagram can be well-understood by the rotations of pseudospin orientation under the magnetic field $h = 2\mu$. At $n = 0$, h is large along the $-\hat{z}$ direction so that all the pseudospins are completely polarized. As n increases, the magnitude

of h decreases so that the pseudospins gradually rotate upward with one of the pseudospins ($\vec{\eta}(A)$) having much faster rotating rate. They become fully polarized again as arriving at the CDW insulating state at $n = \frac{2}{3}$ with $\eta^z(A)$ reaching the maximal value $+\frac{1}{2}$ and both $\eta^z(B)$ and $\eta^z(C)$ reaching minimal value $-\frac{1}{2}$. As n increases further, since $\eta^z(A)$ can not increase anymore, $\vec{\eta}(B)$ and $\vec{\eta}(C)$ gradually turn upward leaving $\vec{\eta}_A$ unchanged. After a critical value $n_c \sim 0.7$, all the pseudospins start to rotate simultaneously and continuously evolve from (D) to (F) in Fig. 3. This continuous evolution of the ground state is not present in the AAFHM since its ground state is ferrimagnetic at zero field. This deviation is because the AAFHAM model is only justified at the strong coupling limit. The larger kinetic energy in this region leads to the less stringent assumption of the strong-coupling. Consequently, the quantum fluctuations arising from the singly occupied states are enhanced, which are in disfavor of CDW but in favor of uniform superfluidity. The continuous evolution also explains why there is no jump at $n = 1$ in Fig. 2. Finally, the rest part of the phase diagram can be easily understood by rotating all the pseudospins upward, and eventually all the pseudospins are fully polarized along $+\hat{z}$ direction at $n = 2$.

One remarkable feature in Fig. 3 is that for a wide region of n ($0.67 \leq n \leq 0.7$, $1 \leq n \leq 1.3$), we find $\langle G|\eta_x(A)|G\rangle = 0$ and $\langle G|\eta_x(B)|G\rangle = -\langle G|\eta_x(C)|G\rangle = \Delta$. As shown in Fig. 4(a), for this type of solutions the pairing order parameters in the real space change signs under 60° rotation with respect to the center chosen to be one site of sublattice A, indicating that the pairing symmetry is in fact f -wave. To confirm the f -wave symmetry, we calculate the intra-band pairing functions Δ_{nn} in the momentum space by projecting the pairing potential in Eq. 4 to the band eigen-basis as:

$$\sum'_{\vec{k}} \sum_{m,n=1}^6 \Delta_{nm}^*(\vec{k}) \psi_n(\vec{k}) \psi_m(-\vec{k}) + h.c., \quad (7)$$

where

$$\Delta_{nm}(\vec{k}) = [\hat{U}^\dagger(\vec{k}) D(\vec{k}) \hat{U}^*(-\vec{k})]_{nm}, \quad (8)$$

$\hat{U}(\vec{k})$ is the unitary matrix such that $\hat{U}^\dagger(\vec{k}) H_s(\vec{k}) \hat{U}(\vec{k}) = \text{diag.}[E_1(\vec{k}), \dots, E_6(\vec{k})]$, and $H_s(\vec{k})$, $D(\vec{k})$ are given in Eq. 5. We have confirmed that all six intra-band pairing functions have three nodal lines and sign changes under 60° rotation, and Δ_{44} is plotted in Fig. 4(b) for demonstration purpose. Thus this is an unconventional supersolid state of frustrated Cooper pairing with the f -wave pairing symmetry.

We also consider the extreme anisotropy limit of the vanishing π -bonding strength, i.e., $t_\perp = 0$. The bond superexchange only results in the J_z -term at the second order perturbation level in Eq. 3. The leading order of the hopping of the Cooper pairs occurs through the

three-site ring exchange

$$\Delta H = - \sum_{ijk} J' [\eta_x(i)\eta_x(j) + \eta_y(i)\eta_y(j)]\eta_z(k) \quad (9)$$

where $J' = \frac{9}{2} \frac{t_\perp^3}{U^2}$. The hopping is frustrated for a plaquette with only one site occupied, but it is unfrustrated for a plaquette with two sites occupied. This means that at low fillings the phase diagram does not change much from the case of nonzero t_\perp , while the system finally evolves to a uniform pairing phase at n close 2. A more detailed analysis will be presented in a later publication.

In summary, we introduce the concept of “frustrated Cooper pairing” of spinless fermions in the p -orbital band in optical lattices. The frustration occurs naturally from the odd parity of the p -orbitals and is a new feature of orbital physics. Exotic supersolid states of Cooper pairs with nonuniform distributions of pair density and phase are obtained with an unconventional f -wave symmetry. This opens up a new opportunity to study the physics of frustrated magnet by using the pseudo-spin algebra of the charge and pair degrees of freedom of Cooper pairs. This idea can also be applied to other even more frustrated lattices, such as Kagome and pyrochlore. In considering the possibility of the existence of exciting spin liquid states therein, their counterparts in terms of “frustrated Cooper pairs” is another interesting direction for further exploration.

C. W. thanks J. Hirsch for helpful discussions. C. W., H. H. H, and W. C. L are supported by the Sloan Research Foundation, ARO-W911NF0810291 and NSF-DMR-03-42832.

Note added Upon the completion of this manuscript, we learned the work by Cai *et al.* [22] in which a similar problem in the square lattice is investigated.

- [1] H. T. Diep, *FRUSTRATED SPIN SYSTEMS* (World Scientific, Singapore, 2005).
- [2] G. Misguich, arXiv.org:0809.2257, 2008.
- [3] R. Moessner and K. S. Raman, arXiv.org:0809.2257, 2008.
- [4] E. Berg, E. Fradkin, and S. A. Kivelson, Physical Review B **79**, 064515 (2009).
- [5] E. Berg, E. Fradkin, S. A. Kivelson, and J. Tranquada, arXiv.org:0901.4826, 2009.
- [6] T. Müller, S. Fölling, A. Widera, and I. Bloch, Phys. Rev. Lett. **99**, 200405 (2007).
- [7] A. Isacsson and S. M. Girvin, Phys. Rev. A **72**, 053604 (2005).
- [8] W. V. Liu and C. Wu, Phys. Rev. A **74**, 13607 (2006).
- [9] C. Wu, W. V. Liu, J. E. Moore, and S. Das Sarma, Phys. Rev. Lett. **97**, 190406 (2006).
- [10] C. Wu, Mod. Phys. Lett. B **23**, 1 (2009).
- [11] C. Wu, D. Bergman, L. Balents, and S. D. Sarma, Phys. Rev. Lett. **99**, 70401 (2007).
- [12] C. Wu and S. D. Sarma, Phys. Rev. B **77**, 235107 (2008).

- [13] S. Z. Zhang, H. H. Hung, and C. Wu, arXiv.org:0805.3031, 2008.
- [14] C. Wu, Phys. Rev. Lett. **100**, 200406 (2008).
- [15] C. Wu, Phys. Rev. Lett. **101**, 186807 (2008).
- [16] W.-C. Lee, C. Wu, and S. Das Sarma, arXiv.org:0905.1146, 2009.
- [17] C. Becker, P. Soltan-Panahi, J. Kronjager, S. Stellmer, K. Bongs, and K. Sengstock, Lasers and Electro-Optics, 2007 and the International Quantum Electronics Conference, 2007.
- [18] A. E. Feiguin and M. P. A. Fisher, Phys. Rev. Lett. **103**, 025303 (2009).
- [19] H. C. Jiang, M. Q. Weng, Z. Y. Weng, D. N. Sheng, and L. Balents, Phys. Rev. B **79**, 020409 (2009).
- [20] F. Wang, F. Pollmann, and A. Vishwanath, Phys. Rev. Lett. **102**, 017203 (2009).
- [21] S. Miyashita, J. Phys. Soc. Jpn. **55**, 3605 (1986).
- [22] Z. Cai *et al.*, arxiv:0910.0508.